Photothermal Release

DOI: 10.1002/ange.200805303

An Efficient Method Based on the Photothermal Effect for the Release of Molecules from Metal Nanoparticle Surfaces**

Amir Bahman Samsam Bakhtiari, Dennis Hsiao, Guoxia Jin, Byron D. Gates,* and Neil R. Branda*

New methods for the spatially and temporally controlled delivery of chemical and/or biochemical species using low-energy visible light offers greater opportunities in photodynamic therapy,[1] chemical synthesis,[2] and photolithography.[3] The fact that designer metal nanoparticles absorb light of specific frequencies (at their plasmon resonance) and efficiently convert it into heat (through the photothermal effect) is a particularly appealing phenomenon that has been effectively used to trigger cell death[4] and melt ice[5] within the vicinity of the nanoparticles. However, to date, the heat generated when visible light is absorbed by such structures has not been used to initiate delivery events. This is surprising, as this technique would provide a convenient and general method to break chemical bonds and release biologically relevant payloads from the nanoparticle surfaces. Both detrimental (poisonous) and beneficial (therapeutic) agents could be released on command by using such a universal method.

We recently set out to develop a new method to harness the local heat that dissipates from the nanoparticles when they are stimulated with visible light, in order to trigger thermally activated bond-breaking reactions close to the nanoparticle surfaces without significantly increasing the temperature of the surrounding environment. This approach has a benefit over others in that specific agents can be delivered to a cell without damaging it. Herein, we describe how we can trigger the release of a fluorescent dye from core–shell nanoparticles as the first illustration of a generalized approach to photothermal release.

We chose the retro-Diels–Alder reaction to demonstrate our new release method because the temperature at which it is activated can be easily tuned by modifying the structure of the two chemical components (the diene and dienophile).[6] This cycloaddition reaction is particularly well-suited for surface-localized chemistry and has been used to selectively decorate[7] and control nanoparticle aggregation[8] by directly applying heat to suspensions of nanoparticles. The photothermal effect has yet to be taken advantage of in this context. We identified a specific retro-Diels–Alder reaction (shown in the substructure in Figure 1 a). Our choice was based on the fact that the bond-breaking reaction of 7-oxa-bicyclo-[2.2.1]hept-5-ene-2,3-dicarboxylic imide to release a furan and a maleimide component barely occurs at room temperature but proceeds above 60 °C. Model studies on both the *endo* and *exo* isomers of the depicted bicyclic system suggest that, as expected, the use of the former isomer is advantageous[9–11] since is cleanly converts into its two components at

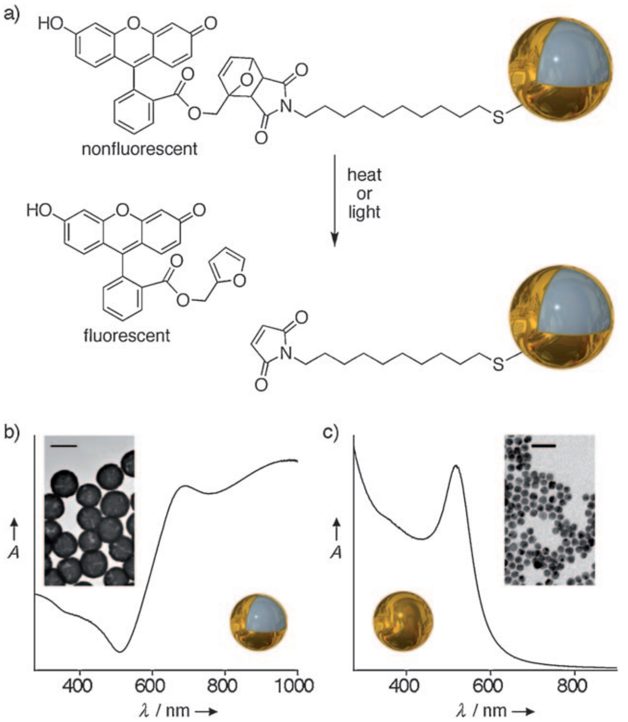

Figure 1. a) Release of the fluorescein dye from the surface of a silica–gold core–shell nanoparticle by using the photothermal effect to induce the retro-Diels–Alder reaction of an anchored 7-oxa-bicyclo-[2.2.1]hept-5-ene-2,3-dicarboxylic imide derivative. UV/Vis absorption spectra of aqueous dispersions with TEM images of each type of particle shown as insets: b) 200 nm diameter core–shell gold nanoparticles (inset scale bar 200 nm)and c) 16 nm diameter solid gold nanoparticles (inset scale bar 50 nm).

---

[*] A. B. S. Bakhtiari, D. Hsiao, G. Jin, Prof. B. D. Gates, Prof. N. R. Branda
4D LABS at Simon Fraser University
8888 University Drive, Burnaby, BC V5A 1S6 (Canada)
Fax: (+1) 778-782-3765
E-mail: bgates@sfu.ca
nbranda@sfu.ca

[**] This research was supported by the Natural Sciences and Engineering Research Council (NSERC) of Canada, the Canada Research Chairs Program, and Simon Fraser University (SFU) through the Community Trust Endowment Fund. This work made use of 4D LABS shared facilities supported by the Canada Foundation for Innovation (CFI), British Columbia Knowledge Development Fund (BCKDF), and Simon Fraser University. We thank Prof. Gary Leach (SFU, Chemistry Department) for helpful discussions and for access to his laser spectroscopy laboratory.

Supporting information for this article is available on the WWW under http://dx.doi.org/10.1002/anie.200805303.

lower temperatures (63 % yield after 5 h for the *endo* isomer compared to 45 % after 8 h for its *exo* counterpart) with no observable side-products.[12] In our example, the bicyclic system has a fluorescein dye attached to the furan component; the dye acts as a useful read-out signal that can be easily detected owing to its high fluorescence quantum efficiency and emission of light in the visible region of the electromagnetic spectrum.

Conveniently, the fluorescence emission from the dye molecule is efficiently quenched by the gold layer surrounding the core–shell nanoparticle as long as it is kept close to the surface of the metal.[13,14] As soon as the dye is released from the nanoparticle surface, fluorescence quenching is reduced and the emission is turned "on", which provides a means to monitor the success of the photothermally induced retro-Diels–Alder reaction by comparing the fluorescence before and after stimulation. The role of the maleimide component is to anchor the bicyclic system to the nanoparticle surface through the Au–S bond that is provided by a long-chain alkane thiol (the synthesis of the fluorescent bicyclic system is described in the Supporting Information). A core–shell metal nanoparticle, in which a thin layer of gold is wrapped around a silica sphere, is shown in Figure 1 a.[15] The use of a solid gold nanoparticle[16,17] for photothermal release is also described.

As mentioned above, the photothermal process leads to the radiation of heat from the surface of metal nanoparticles as a result of phonon relaxation from an excited state that is accessed by irradiation of the surface plasmon resonance (SPR) band of the nanoparticle.[18–20] The position of the SPR band in the electromagnetic spectrum is dictated by the size, shape, and composition of the nanoparticles, all of which can be programmed into the nanoparticle synthesis.[21] SPR bands typically appear within the visible and near-infrared (NIR) regions of the spectrum (from 400 nm to greater than 1100 nm),[22] with the longer wavelengths being favorable in release applications (especially biomedical-related), since lower energy light will penetrate deeper into tissue while minimizing damage to the surroundings. The longer wavelengths are also less efficiently absorbed by the dielectric coating of the nanoparticle surface or by the medium in which the particles are dispersed.[23,24] Our studies focus on the use of decorated core–shell nanoparticles ((200 ± 10) nm diameter) that are composed of silica spheres wrapped in a (10 ± 2) nm thick shell of gold and have two SPR bands (700 and 1000 nm) in the NIR region of the spectrum (Figure 1 b). The synthesis of these particles started with the preparation of silica colloids by a modified Stöber technique,[25] followed by attachment of an amino-terminated silane to the surface of the SiO_2 particles.[26] This surface modification is necessary in order to attach the 3 nm diameter gold seeds[27] onto the spherical silica templates needed to initiate the growth of the 10 nm thick gold shell by reduction of tetrachloroauric acid.[15] The optical properties of solid gold nanoparticles with a diameter of (16 ± 3) nm are shown in Figure 1 c, which illustrates how the SPR band is significantly shifted to higher energy (520 nm) because of the nanoparticle size and composition. These pure gold nanoparticles are synthesized in one step by a thermally induced reduction of tetrachloroauric acid with trisodium citrate.[16,17] Both syntheses produce stable aqueous dispersions of the respective nanoparticles and transmission electron microscopy (TEM) images reveal that both types of particles have monodisperse shapes and sizes (see insets in Figure 1 b and Figure 1 c).

The 200 nm diameter gold nanoparticles were functionalized with the fluorescein dye by treating aqueous nanoparticle suspensions with an excess of the bicyclic retro-Diels–Alder system in its disulfide form.[28,29] The reaction mixtures were best left to equilibrate overnight at 4 °C to ensure maximum coverage of the nanoparticle surface with the organic system through formation of Au–S bonds. Any excess bicyclic disulfide could be removed by repeated centrifugation–resuspension (using 18 MΩ water) cycles[30] until all free fluorescein (not bound to the nanoparticles) was removed (as monitored by fluorescence spectroscopy).[31] The final suspension[32] of decorated nanoparticles retained only a very low level of emission, which arose from the quenching of the dye's fluorescence through photoinduced energy transfer to the nanoparticle,[33] thus providing a useful baseline with which the release event can be monitored (Figure 2 a).

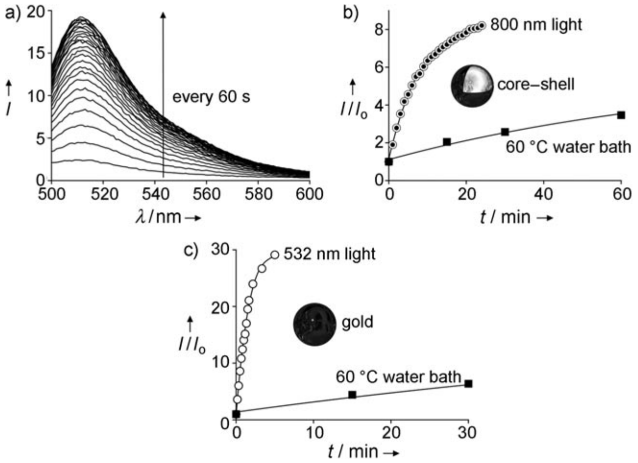

Figure 2. a) Representative spectra showing changes in the fluorescence intensity when an aqueous dispersion of 200 nm diameter gold-coated silica nanoparticles functionalized with the fluorescein dye is irradiated with NIR light (800 nm, 1 kHz, 700 mW, 100 fs). Increase in fluorescence intensity when aqueous dispersions of b) 200 nm core–shell and c) 16 nm solid gold nanoparticles decorated with the fluorescein dye are heated in a water bath at 60 °C (■) or irradiated with 800 nm light (1 kHz, 700 mW, 100 fs) for the core–shell particles (⊙) and 532 nm light (10 Hz, 100 mW, 4 ns) for the gold nanoparticles (○).

The fluorescence intensity of the fluorescein dye immediately increased when aqueous dispersions of the core–shell nanoparticles were irradiated at 800 nm (1 kHz, 700 mW, 100 fs) with a pulsed laser light that overlaps with their SPR band. This increase indicates effective release of the dye into the bulk solution. A representative example of the changes typically observed is shown in Figure 2 a. During this process, there was no measurable change in temperature of the aqueous suspension measured by using a thermocouple, even though there was clearly enough heat generated at the surface of the nanoparticles to break the bonds in the retro-Diels–

Alder system. No changes in fluorescence intensity were observed when a similar suspension is exposed to ambient light, since this light source is insufficient to induce the retro-Diels–Alder reaction through the photothermal effect. The increase in fluorescence intensity was significantly more rapid when the retro-Diels–Alder reaction is triggered with 800 nm pulsed light than when it is induced by applying direct heat (Figure 2b).

The photothermally induced release was almost complete after only 30 min, while the equivalent release reaction progressed to only a quarter of this extent when an identical sample was incubated in a water bath at 60 °C, a temperature at which significant damage to cellular systems would occur. Similar trends were observed for the 16 nm gold nanoparticles when 532 nm light (10 Hz, 100 mW, 4 ns) was used (Figure 2c). Once again, the photothermal release from the nanoparticles is significantly more efficient than when the sample was directly heated. We estimate that approximately 1600 dye molecules are released per gold nanoparticle.[34]

Initial inspection of Figure 2b,c suggests that the release of the fluorescein dye from the 16 nm gold nanoparticles is more efficient than the release observed for the core–shell particles, therefore the former is preferable. This is in fact not the case, and a closer look at the results suggests that there is substantial cleavage of the Au–S bond during the photothermal event. As observed for other systems, a blue shift occurred in the SPR band when the 16 nm particles were irradiated with 532 nm pulsed light (Figure 3a). This shift correlates to the loss of the surface-capping group,[35] and is not observed when the particles were directly heated. On the other hand, the position, intensity, and shape of the SPR bands recorded for the core–shell nanoparticles were consistent, even after more than 17 min of irradiation with 800 nm light (Figure 3b). A significant increase in fluorescence intensity was observed during this period of irradiation. These results indicate a different mechanism for the photothermal release of the fluorescein dye from each of the two types of gold nanoparticles. The photothermal effect most likely leads to the release of the dye from the 16 nm gold nanoparticle through a combination of Au–S bond cleavage and the retro-Diels–Alder reaction. The lack of an observed shift in the SPR band following photothermal release from the core–shell particles suggests that the retro-Diels–Alder reaction is the dominant release mechanism from these particles.

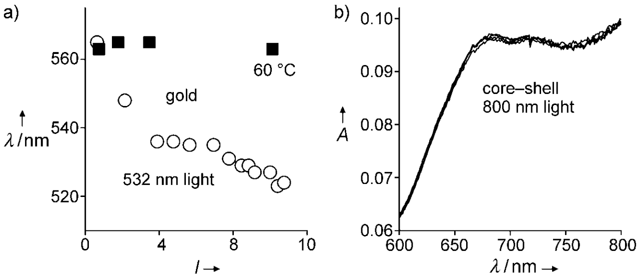

Figure 3. a) Changes in absorption maximum as the fluorescence intensity increases when aqueous dispersions of 16 nm gold nanoparticles decorated with the fluorescein dye are heated in a water bath at 60 °C (■) or irradiated with 532 nm light (10 Hz, 100 mW, 4 ns) (○). b) Absorption spectra of an aqueous dispersion of 200 nm core–shell nanoparticles decorated with the fluorescein dye irradiated with NIR light (800 nm, 1 kHz, 700 mW, 100 fs) over a period of 17 min. Minimal changes are observed over this period.

The examples presented herein clearly demonstrate that the localized heat generated by the photothermal effect of metal nanoparticles can be harnessed to selectively break chemical bonds and release anchored components. The release event can be visually demonstrated by using fluorescence microscopy to compare aqueous samples of core–shell nanoparticles before and after irradiation. Figure 4 clearly illustrates how aqueous dispersions of both the decorated and nondecorated 200 nm core–shell nanoparticles do not significantly fluoresce until they are exposed to pulsed 800 nm light. The rate of photothermally induced release from the core–shell nanoparticle is approximately four times that observed for a thermally initiated release. Results obtained from irradiation of a solid gold nanoparticle with visible light suggest that the dye molecules are released through the breakage of Au–S bonds. This type of release is, however, viewed as detrimental to biological systems, as free thiols are unstable and can lead to unwanted side-reactions. Future studies will take advantage of the demonstrated selective release of a molecular payload, and explore the possibilities for both temporal and spatial control of release. This on-demand release of a molecular payload will be highly beneficial to drug delivery and other biomedical applications.

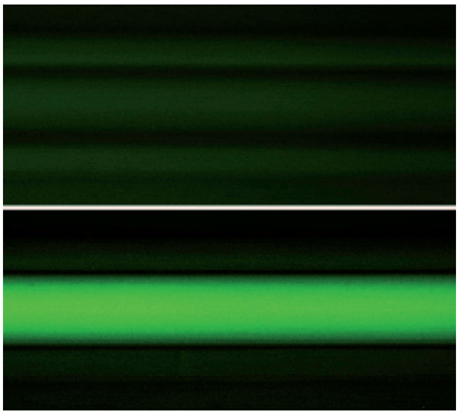

Figure 4. Fluorescence microscopy images of capillary tubes containing 200 nm diameter core–shell particles decorated with the fluorescein dye before (top) and after (bottom) irradiation with light (800 nm, 1 kHz, 700 mW, 100 fs) for 10 min.

Received: October 29, 2008
Revised: March 29, 2009
Published online: April 30, 2009

Keywords: cycloaddition · fluorescence · nanostructures · photorelease · photothermal effects

---

[1] T. Patrice, *Photodynamic Therapy*, Royal Society of Chemistry, Cambridge, **2003**.

[2] W. M. Horspool, F. Lenci, *CRC Handbook of Organic Photochemistry and Photobiology*, *Vols. 1 and 2*, Routledge, USA, **2003**.

[3] S. P. A. Fodor, J. L. Read, M. C. Pirrung, L. Stryer, A. T. Lu, D. Solas, *Science* **1991**, *251*, 767 – 773.

[4] C. M. Pitsillides, E. K. Joe, X. Wei, R. R. Anderson, C. P. Lin, *Biophys. J.* **2003**, *84*, 4023 – 4032.

[5] H. H. Richardson, Z. N. Hickman, A. O. Govorov, A. C. Thomas, W. Zhang, M. E. Kordesch, *Nano Lett.* **2006**, *6*, 783 – 788.

[6] V. Lemieux, S. Gauthier, N. R. Branda, *Angew. Chem.* **2006**, *118*, 6974 – 6978; *Angew. Chem. Int. Ed.* **2006**, *45*, 6820 – 6824.

[7] M. Shi, J. H. Wosnick, K. Ho, A. Keating, M. S. Shoichet, *Angew. Chem.* **2007**, *119*, 6238 – 6243; *Angew. Chem. Int. Ed.* **2007**, *46*, 6126 – 6131.

[8] J. Zhu, A. J. Kell, M. S. Workentin, *Org. Lett.* **2006**, *8*, 4993 – 4996.

[9] K. Adachi, A. K. Achimuthu, Y. Chujo, *Macromolecules* **2004**, *37*, 9793 – 9797.

[10] J. R. McElhanon, D. R. Wheeler, *Org. Lett.* **2001**, *3*, 2681 – 2683.

[11] The *exo* isomer converts to its furan and maleimide components at higher temperatures.

[12] See the Supporting Information.

[13] N. Nerambourg, M. H. V. Werts, M. Charlot, M. Blanchard-Desce, *Langmuir* **2007**, *23*, 5563 – 5570.

[14] F. Cannone, G. Chirico, A. R. Bizzarri, S. Cannistraro, *J. Phys. Chem. B* **2006**, *110*, 16491 – 16498.

[15] T. Pham, J. B. Jackson, N. J. Halas, T. R. Lee, *Langmuir* **2002**, *18*, 4915 – 4920.

[16] B. V. Enüstün, J. Turkevich, *J. Am. Chem. Soc.* **1963**, *85*, 3317 – 3328.

[17] J. Kimling, M. Maier, B. Okenve, V. Kotaidis, H. Ballot, A. Plech, *J. Phys. Chem. B* **2006**, *110*, 15700 – 15707.

[18] C. K. Sun, F. Vallée, L. Acioli, E. P. Ippen, J. G. Fujimoto, *Phys. Rev. B* **1993**, *48*, 12365 – 12368.

[19] T. S. Ahmadi, S. L. Logunov, M. A. El-Sayed, *J. Phys. Chem.* **1996**, *100*, 8053 – 8056.

[20] B. Khlebtsov, V. Zharov, A. Melnikov, V. Tuchin, N. Khlebtsov, *Nanotechnology* **2006**, *17*, 5167 – 5179.

[21] P. K. Jain, K. S. Lee, I. H. El-Sayed, M. A. El-Sayed, *J. Phys. Chem. B* **2006**, *110*, 7238 – 7248.

[22] C. H. Chou, C. D. Chen, C. R. C. Wang, *J. Phys. Chem. B* **2005**, *109*, 11135 – 11138.

[23] L. R. Hirsch, R. J. Stafford, J. A. Bankson, S. R. Sershen, B. Rivera, R. E. Price, J. D. Hazle, N. J. Halas, J. L. West, *Proc. Natl. Acad. Sci. USA* **2003**, *100*, 13549 – 13554.

[24] A. M. Gobin, M. H. Lee, N. J. Halas, W. D. James, R. A. Drezek, J. L. West, *Nano Lett.* **2007**, *7*, 1929 – 1934.

[25] W. Stöber, A. Fink, E. Bohn, *J. Colloid Interface Sci.* **1968**, *26*, 62 – 69.

[26] A. van Blaaderen, A. Vrij, *J. Colloid Interface Sci.* **1993**, *156*, 1 – 18.

[27] D. G. Duff, A. Baiker, P. P. Edwards, *Langmuir* **1993**, *9*, 2301 – 2309.

[28] The disulfide used to decorate the nanoparticles is not symmetrical and has one bicyclic system and one free maleimide derivative attached to it.

[29] A. Ulman, *Chem. Rev.* **1996**, *96*, 1533 – 1554.

[30] Purification of the particles included at least three complete cycles of centrifugation with decanting of the supernatant followed by dispersion of the collected solids in 18 MΩ water. The centrifugation step required a speed of 10000 rpm for 10 min for the gold nanoparticles and 4000 rpm for 10 min for the core–shell nanoparticles.

[31] Typically, the fluorescence emission intensity remained constant after three purification cycles, which indicated that the unbounded dye had been removed from the reaction.

[32] A time dependent study on the nanoparticles dispersed in water (Figure S7 in Supporting Information) indicated a relatively stable dispersion of gold nanoparticles over a period of 4 h. These dispersions are stable for time periods longer than the length of the photothermal release experiments.

[33] K. G. Thomas, B. I. Ipe, P. K. Sudeep, *Pure Appl. Chem.* **2002**, *74*, 1731 – 1738.

[34] The number of fluorescent molecules per particle was estimated based on a quantitative analysis of the amount of dye released and the number of particles in solution. For this experiment, a dispersion of dye-coated nanoparticles was adjusted to pH 12 and heated to 80 °C in a water bath. The presence of a strong base (e.g., KOH) efficiently hydrolyzes the ester linkage in the dye bound to the nanoparticles. The release of dye molecules was monitored by fluorescence spectroscopy. Upon reaching a plateau in the overall fluorescence emission, the quantity of dye released was determined using a series of fluorescein standards. This quantitative analysis provided an estimate of the number of dye molecules released into solution. The number of gold nanoparticles in solution was quantified using the average particle size, the density of gold, and the amount of gold in solution (as determined by inductively coupled plasma MS analysis).

[35] P. K. Jain, W. Qian, M. A. El-Sayed, *J. Am. Chem. Soc.* **2006**, *128*, 2426 – 2433.